Oxygen Transport Ceramic Membranes

Quarterly Report

October 2003 – December 2003

Principal Authors:

Prof. S. Bandopadhyay

Dr. N. Nagabhushana

Issued: February 2004

DOE Award # DE-FC26-99FT40054

School of Mineral Engineering,
University of Alaska Fairbanks
Fairbanks, AK 99775

Contributing sub contractors:

1. **Dr. X.-D Zhou, W. B. Yelon, and Prof. H. U. Anderson**; Materials Research Center, University of Missouri-Rolla, Rolla, MO 65401
2. **Prof. Alan Jacobson and Prof. C.A. Mims;** University of Houston/University of Toronto

DISCLAIMER

ABSTRACT

The present quarterly report describes some of the investigations on the structural properties of dense OTM bars provided by Praxair and initial studies on newer composition of Ti doped LSF.

Dense OTM bars provided by Praxair were loaded to fracture at varying stress rates. Studies were done at room temperature in air and at 1000ºC in a specified environment to evaluate slow crack growth behavior. In addition, studies were also begun to obtain reliable estimates of fracture toughness and stable crack growth in specific environments.

Newer composition of Ti doped LSF membranes were characterized by neutron diffraction analysis. Quench studies indicated an apparent correlation between the unit cell volume and oxygen occupancy. The studies however, indicated an anomaly of increasing Fe/Ti ratio with change in heat treatment. Ti doped LSF was also characterized for stoichiometry as a function of temp and pO_2. The non stoichiometry parameter δ was observed to increase almost linearly on lowering pO_2 until a ideal stoichiometric composition of $\delta = 0.175$ was approached.

TABLE OF CONTENTS

LIST OF GRAPHICAL MATERIALS

INTRODUCTION

Conversion of natural gas to liquid fuels and chemicals is a major goal for the Nation as it enters the 21st Century. Technically robust and economically viable processes are needed to capture the value of the vast reserves of natural gas on Alaska's North Slope, and wean the Nation from dependence on foreign petroleum sources. Technologies that are emerging to fulfill this need are all based syngas as an intermediate. Syngas (a mixture of hydrogen and carbon monoxide) is a fundamental building block from which chemicals and fuels can be derived. Lower cost syngas translates directly into more cost-competitive fuels and chemicals.

The currently practiced commercial technology for making syngas is either steam methane reforming (SMR) or a two-step process involving cryogenic oxygen separation followed by natural gas partial oxidation (POX). These high-energy, capital-intensive processes do not always produce syngas at a cost that makes its derivatives competitive with current petroleum-based fuels and chemicals.

In the mid 80's BP invented a radically new technology concept that will have a major economic and energy efficiency impact on the conversion of natural gas to liquid fuels, hydrogen, and chemicals.[1] This technology, called Electropox, integrates oxygen separation with the oxidation and steam reforming of natural gas into a single process to produce syngas with an economic advantage of 30 to 50 percent over conventional technologies.[2]

The Electropox process uses novel and proprietary solid metal oxide ceramic oxygen transport membranes [OTMs], which selectively conduct both oxide ions and electrons through their lattice structure at elevated temperatures.[3] Under the influence of an oxygen partial pressure gradient, oxygen ions move through the dense, nonporous membrane lattice at high rates with 100 percent

---

[1]Mazanec, T. J.; Cable, T. L.; Frye, J. G., Jr.; US 4,793,904, 27 Dec **1988**, assigned to The Standard Oil Company (now BP America), Mazanec, T. J.; Cable, T. L.; US 4,802,958, 7 Feb **1989**, assigned to the Standard Oil Co. (now BP America), Cable, T. L.; Mazanec, T. J.; Frye, J. G., Jr.; European Patent Application 0399833, 24 May **1990**, published 28 November **1990.**

[2]Bredesen, R.; Sogge, J.; "A Technical and Economic Assessment of Membrane Reactors for Hydrogen and Syngas Production" presented at Seminar on the Ecol. Applic. of Innovative Membrane Technology in the Chemical Industry", Cetraro, Calabria, Italy, 1-4 May **1996**.

[3]Mazanec, T.J., *Interface*, **1996**; Mazanec, T.J., *Solid State Ionics*, 70/71, **1994** 11-19; "Electropox: BP's Novel Oxidation Technology", T.J. Mazanec, pp 212-225, in "The Role of Oxygen in Improving Chemical Processes", M. Fetizon and W.J. Thomas, eds, Royal Society of Chemistry, London, **1993**; "Electropox: BP's Novel Oxidation Technology", T.J. Mazanec, pp 85-96, in "The Activation of Dioxygen and Homogeneous Catalytic Oxidation", D.H.R. Barton, A. E. Martell, D.T. Sawyer, eds, Plenum Press, New York, **1993**; "Electrocatalytic Cells for Chemical Reaction", T.J. Mazanec, T.L. Cable, J.G. Frye, Jr.; Prep Petrol Div ACS, San Fran, **1992** *37*, 135-146; T.J. Mazanec, T.L. Cable, J.G. Frye, Jr.; *Solid State Ionics*, **1992**, 53-56, 111-118.

selectivity. Transported oxygen reacts with natural gas on the fuel side of the ceramic membrane in the presence of a catalyst to produce syngas.

In 1997 BP entered into an OTM Alliance with Praxair, Amoco, Statoil and Sasol to advance the Electropox technology in an industrially sponsored development program. These five companies have been joined by Phillips Petroleum and now are carrying out a multi-year $40+ million program to develop and commercialize the technology. The program targets materials, manufacturing and engineering development issues and culminates in the operation of semi-works and demonstration scale prototype units.

The Electropox process represents a truly revolutionary technology for conversion of natural gas to synthesis gas not only because it combines the three separate unit operations of oxygen separation, methane oxidation and methane steam reforming into a single step, but also because it employs a chemically active ceramic material in a fundamentally new way. On numerous fronts the commercialization of Electropox demands solutions to problems that have never before been accomplished. Basic problems in materials and catalysts, membrane fabrication, model development, and reactor engineering all need solutions to achieve commercial success.

Six important issues have been selected as needing understanding on a fundamental level at which the applied Alliance program cannot achieve the breadth and depth of understanding needed for rapid advancement. These issues include:

1. Oxygen diffusion kinetics (University of Houston);
2. Phase stability and stress development (University of Missouri - Rolla);
3. Mechanical property evaluation in thermal and chemical stress fields (University of Alaska Fairbanks)

Statement of Work

Task 1 *Evaluate phase stability and thermal expansion of candidate perovskite membranes and develop techniques to support these materials on porous metal structures.*

Task 2 *Determine materials mechanical properties under conditions of high temperatures and reactive atmospheres.*

Task 3 *Measure kinetics of oxygen uptake and transport in ceramic membrane materials under commercially relevant conditions using isotope labeling techniques.*

EXECUTIVE SUMMARY

Research on the Oxygen Transport Membranes as listed as tasks 1-3 are being performed at the various universities under the stewardship of Praxair. The quarterly technical report presents the progress of the various tasks defined to understand the fundamental concepts and structural performance of the ceramic membrane in realistic conditions.

Refinement studies of the neutron data on Ti^{3+} doped $La_{0.6}Sr_{0.4}FeO_{3-\delta}$ showed no evidence for antiferromagnetic ordering. Ideally, the Fe/Ti ratio should refine to a constant value, while the oxygen occupancy varies according to treatment conditions. The deviation from cubicity is extremely small at all temperatures and suggests that the refined deviation from cubic symmetry may be an artifact of the refinement. In addition, the data indicates that the Fe/Ti ratio apparently changes with heat treatment which is physically possible if there is phase separation (which is not observed in the neutron data).

Dense OTM bars were evaluated for slow crack growth (SCG) in air at room temperature and in condition of flowing N_2 switched to air at 1000ºC. The latter condition is representative of the air side of OTM (upon fabrication, stoichiometry of the composition is fixed by cooling in N_2). The SCG parameters n and D were calculated as 23.57, 94.71 and 11.28, 80.2 in air at room temperature and in N_2/Air at 1000ºC respectively. The high value of n = 23.6 at RT, air indicates that the OTM material is not very susceptible to slow crack growth. However, the value of n decreases drastically to 11.3 in N_2/Air (less than 50% at RT) indicating that the OTM material is increasingly prone to SCG. Fracture toughness ($\boldsymbol{K_c}$) of the OTM sample in the specified environment, measured from two techniques indicated reasonable agreement with values approximated from indentation techniques.

The oxygen non-stoichiometry (δ) for $La_{0.2}Sr_{0.8}Fe_{0.55}Ti_{0.45}O_{3-\delta}$ was measured as a function of oxygen partial pressure at $750 \leq T \leq 1040$ °C. Measurements were made in a sealed electrochemical cells at $10^{-16} \leq pO_2 \leq 0.3$ atm. It was noted that the δ-values changed very systematically (total changes in δ were less than ~ 0.1) as a function of temperature and the oxygen partial pressure. The oxygen non-stoichiometric results can be fitted by using polynomial fitting and the results used to investigate the relationships of δ vs. T at constant pO_2 and log pO_2 vs. T at constant δ.

Task 1: Preparation and Characterization of Dense Ceramic oxygen Permeable Membranes

X.-D Zhou[1], Q. Cai[2], J. Yang[1], W. B. Yelon[1], W. J. James[1] and H. U. Anderson[1]

1. **Materials Research Center, University of Missouri-Rolla, Rolla, MO 65401**
2. **Department of Physics, University of Missouri-Columbia, Columbia, MO 65211**

Neutron Diffraction Analysis of $La_{0.2}Sr_{0.8}Fe_{0.55}Ti_{0.45}O_{3-\delta}$ (L2SF55T)

Room temperature neutron diffraction was used to characterize the structural properties of samples of L2SF55T subject to different heat treatments and quenches. Seven samples were studied. Six were heated in air to various temperatures and quenched rapidly to low temperature, while the seventh was slowly cooled to room temperature after heating to 1200ºC. The neutron measurements were carried out using the position sensitive detector – diffractometer at the University of Missouri Research Reactor (MURR) in Columbia, MO.

In comparison to the previously measured samples of $La_{0.6}Sr_{0.4}FeO_{3-\delta}$ (L6SF) no evidence for antiferromagnetic ordering was observed in the diffraction data, i.e., the observed data could be fully fitted without any magnetic contribution. This simplification leads to a higher symmetry space group (R-3c) compared to the P-3/c1 group previously employed, and reduces the number of independent oxygen sites from three to one. Refinement of the neutron data was carried out assuming a fixed La/Sr ratio and allowing the other occupancies to vary (the Fe/Ti ratio and the oxygen occupancy). Ideally, the Fe/Ti ratio should refine to a constant value, while the oxygen occupancy varies according to treatment conditions. In addition to the occupancy parameters, lattice parameters a and c (using a hexagonal setting of the rhombohedral unit cell) and isotropic thermal parameters were allowed to vary.

Table 1 shows the results of the refinements for the seven samples. Rather than present the hexagonal *a* and *c* parameters, the table lists "cubic" parameters, $a = a_h/\sqrt{2}$ and $c = c_h/2\sqrt{3}$ in order to give a simple view of the deviation from cubic symmetry. For the ideal cubic perovskite cell these two parameters should be equal and, indeed, the deviation from cubicity is extremely small at all temperatures. Furthermore the change of the ratio of the "cubic" parameters from $a/c \geq 1$ for the lower temperature treatment to $a/c < 1$ for the

highest temperature, suggests that the refined deviation from cubic symmetry may be an artifact of the refinement. The unit cell volume and refined oxygen occupancy are plotted in figure 1. It can be seen that the both parameters change only slightly between the slowed cooled sample and that quenched from 1000ºC. Both parameters show a marked shift for the 1100ºC quenched sample, and only small (and perhaps not significant) changes at the higher temperatures. It may be necessary to re-measure these samples with better statistics in order to determine if there is an evolution in the unit cell and oxygen occupancy between 1100ºC and 1500ºC. However, the clear correlation between the unit cell volume and oxygen occupancy is expected and equally reflected in the L6SF data. However, in that case, the change in both parameters was less abrupt and showed continued evolution above 1100ºC.

The data, however, contain one anomalous finding, the Fe/Ti ratio apparently changes with heat treatment. This is physically possible if there is phase separation (which is not seen in the neutron data). It may however also be a refinement artifact perhaps arising from improper choice of space group. Further analysis using a variety of space groups including cubic and tetragonal groups will be carried out.

Table 1 Results of the refinements for the six samples quenched to room temperature between 1000°C and 1500°C . The seventh sample was sintered at 1200°C and then slowly cooled to room temperature (3°C /min).

Temp (°C)	**La**	**Sr**	**Fe**	**Ti**	**O**	**Vol (Å^3)**	$a/\sqrt{2}$ **(Å)**	$c/2\sqrt{3}$ **(Å)**
1500	0.19965	0.80465	0.5324	0.47795	2.7588	357.53	3.9042	3.9093
1400	0.19965	0.80465	0.53845	0.4719	2.7951	358.15	3.9088	3.9069
1300	0.19965	0.80465	0.53845	0.46585	2.783	357.25	3.9052	3.9043
1200	0.19965	0.80465	0.55055	0.4598	2.78905	357.6	3.9064	3.9057
1100	0.19965	0.80465	0.5445	0.46585	2.81325	357.401	3.9057	3.9050
1000	0.19965	0.80465	0.5566	0.4477	2.9766	354.844	3.8961	3.8961
RT	0.19965	0.80465	0.56265	0.4477	3.025	354.76	3.8958	3.8958

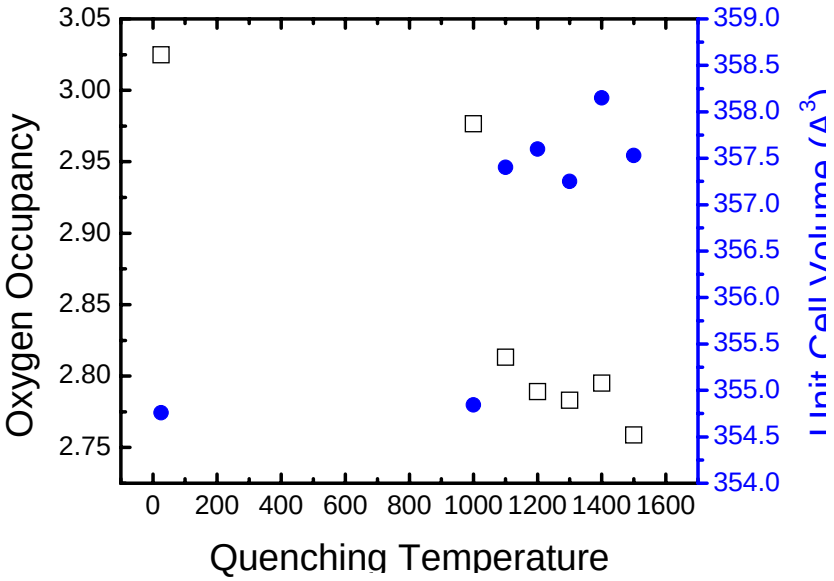

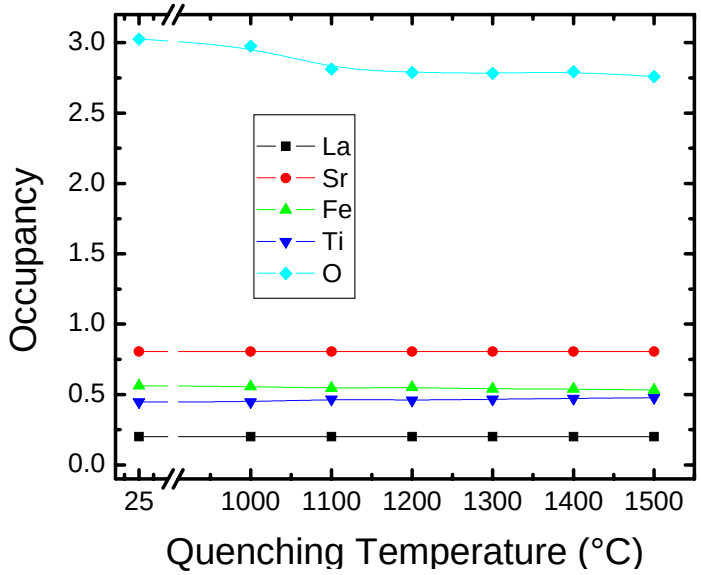

Figure 1 Unit cell volume and refined oxygen occupancy as a function of quench temperature

FUTURE STUDIES:

- To improve neutron diffractometry and Rietveld refinement
- To quench L2SF55T at reducing environments and conducting neutron diffraction measurements
- To initiate the studies to understand the hysteresis curve for LSF and LSCF series
- To study transport and thermal expansion measurements on Ti doped LSF.

TASK 2: Determine material mechanical properties under conditions of high temperature and reactive atmosphere

Prof. Sukumar Bandopadhyay and Dr. Nagendra Nagabhushana
University of Alaska Fairbanks

In this quarter, slow crack growth studies were continued on OTM bar samples received from Praxair. Several approaches were attempted in establishing a methodology to obtain stable crack growth in environmental conditions.

EXPERIMENTAL

21 OTM bars of dimensions 3x4x48 mm were provided by Praxair. The edges of the OTM bars were chamfered prior to testing. As discussed in previous reports, the tests were done in-situ in a autoclave mounted on a servo-electric loading frame. Loading was done in a in-house designed 4 –point flexure with an outer span of 38.1 mm and inner span of 19.05 mm (ASTM D) span. A total of 9 samples were loaded at varying strain rates at room temperaturein air and 8 samples at 1000ºC in an atmosphere of N_2/Air respectively. The stressing rates were so chosen as to provide a minimum of two decades in loading rates and 2 samples were tested at each loading rates. Stable crack growth in the OTM samples were sought to be achieved by loading to fracture a notched beam (Single Edge Notched Beam - SENB) and beam with vickers indents on the surface (Indentation Fracture – IF). The samples were stored for detailed fracture and XRD analysis.

RESULTS AND DISCUSSIONS

Calculation of Fracture Strength:

The fracture strength σ_f, of the OTM bars in 4-point flexure were calculated by the simple beam formula,

Fracture Strength σ_f, MPa = $\dfrac{3PL}{4BW^2}$ Where P = Fracture Load, L = Outer Span, B = thickness and W = width of the beam respectively.

The fracture strength of the bars tested at room temperature in air are listed in table 2 and the load-displacement traces shown graphically in Fig.2.

Table 2 Slow Crack Growth tests in air at Room Temperature

No	Code	Avg, cm	Avg. m	Avg. m	Span, m	Load (N)	Strength (MPa)	Cross Head Speed
2	1b	4.828	0.004	0.003	0.0381	165	114.36	0.01mm/s
3	1c	4.817	0.004	0.003	0.0381	169	111.06	0.01mm/s
4	1d	4.813	0.004	0.003	0.0381	163.6	117.23	0.01 mm/s
5	1e	4.840	0.004	0.003	0.0381	151.6	103.71	0.001mm/s
6	2a	4.839	0.004	0.003	0.0381	157.2	102.76	0.001mm/s
7	2b	4.828	0.004	0.003	0.0381	124.7	92.09	0.0001mm/s
8	2c	4.833	0.004	0.003	0.0381	128.5	92.52	0.0001mm/s
18	3g	4.832	0.004	0.003	0.0381	111	86.09	0.00005mm/s
19	3h	4.838	0.004	0.003	0.0381	116.5	90.70	0.00005mm/s

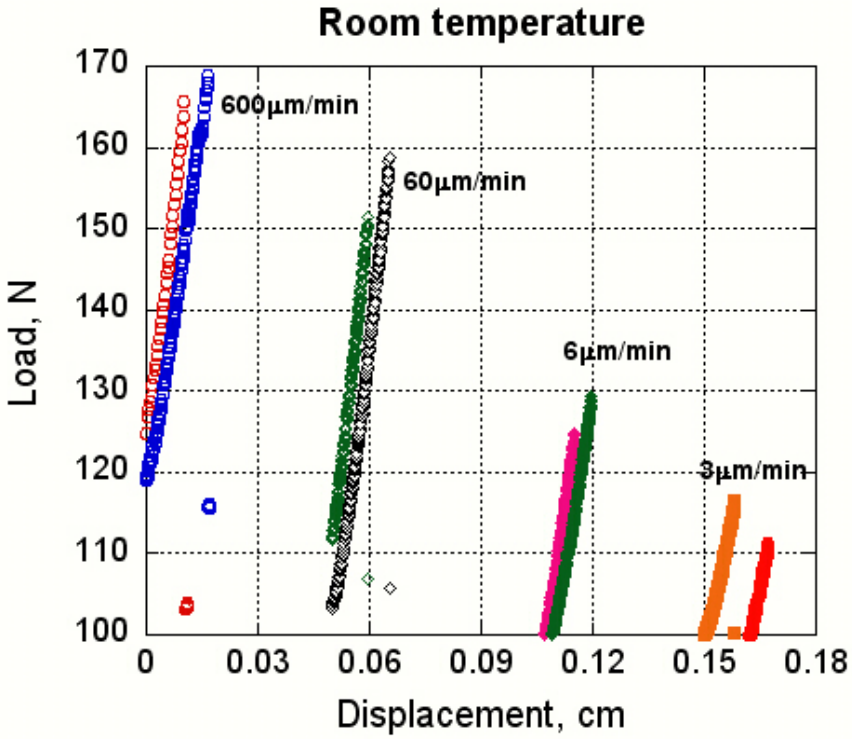

Figure 2 OTM flexural strength tested in varying stress rates at RT in air.

The highest strength of 115 MPa was recorded at the highest cross- head speed of 0.01 mm/s. Thereafter the strength continuously decreased with decreasing cross-head speeds and a low of 86 MPa was recorded at a cross-head speed of 0.00005 mm/s.

Flexural strength in environment:

The OTM bars were load in the fixture and heated in flowing Nitrogen up to 1000ºC. Thereafter, the nitrogen flow was shut off with the outlet fully open. The soaking was for 1 hour prior to application of any load. The bars were loaded at the same cross head speeds as at room temperature. The furnace power was totally shut off after fracture of the sample. A typical test had a heating up period of 2½ hours, soaking of 1 hour, loading rates as specified and a cool down period of 1000-700ºC in 45 min. and 700-200ºC in 1½ hrs for a sum total of 6-7 hours.

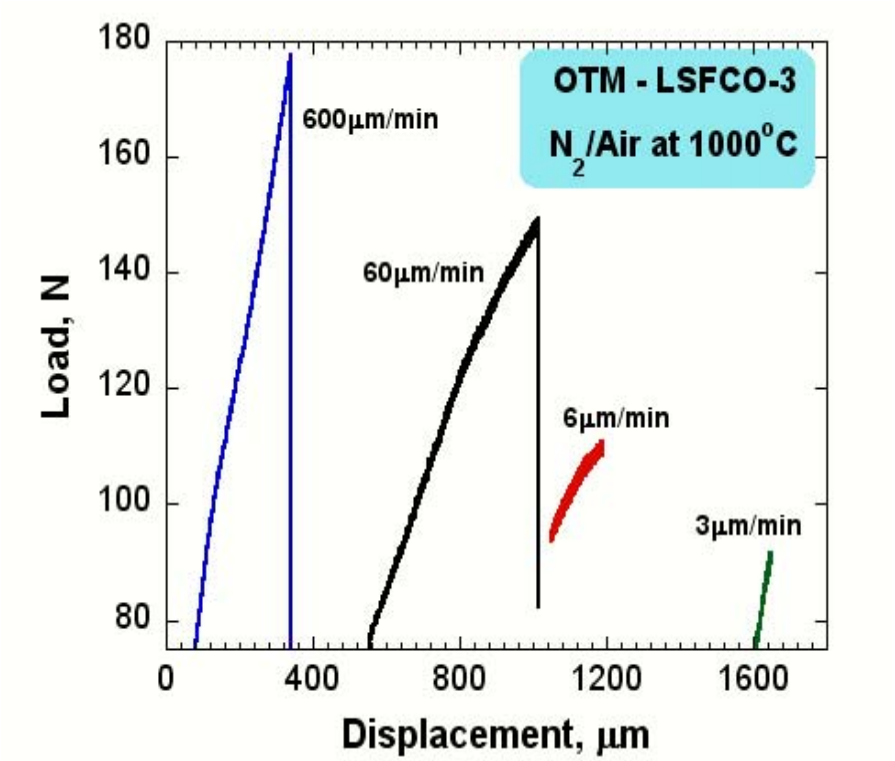

Figure 3 OTM flexural strength at varying stress rates in N_2/Air at 1000ºC.

The flexural strength as calculated from the fracture load discussed in previous section is presented in table 3 and the load-displacement curves graphically plotted in Fig. 3. At high cross-head speeds (0.01 mm/s), the strength (110 and 118 MPa) recorded was comparable to that of at room temperature (so called `inert' strength). Thereafter the strength decreased much steeper as indicated by a recorded strength of 69 MPa at 0.00005 mm/s.

Table 3 Slow Crack Growth tests in N_2/Air at 1000ºC

No	Code	Avg m	Avg m	Avg m	Span m	Load (N)	Strength (MPa)	Cross Head speed
12	3a	0.049	0.0041	0.0032	0.0381	156.6	110.75	0.01mm/s
13	3b	0.049	0.0042	0.0032	0.0381	176.84	118.92	0.01mm/s
14	3c	0.048	0.0041	0.0031	0.0381	126	91.57	0.001 mm/s
15	3d	0.049	0.0042	0.0032	0.0381	148.6	98.49	0.001mm/s
16	3e	0.048	0.0040	0.0031	0.0381	105.7	80.13	0.0001mm/s
17	3f	0.049	0.0041	0.0031	0.0381	110.6	79.78	0.0001mm/s
20	3i	0.049	0.0041	0.0031	0.0381	89.7	66.03	0.00005mm/s
21	3f	0.049	0.0040	0.0031	0.0381	90.2	69.03	0.00005mm/s

Slow Crack Growth analysis in RT (Air) and at 1000ºC (N_2/Air)

From the individual load-displacement traces of the specimen tested, the rate of stress increase was calculated as function of time from the equation: $\dot{\sigma} = \frac{3\dot{P}(S_o - S_i)}{2BW^2}$

Where P is the load rate, B is the specimen thickness, W is the width and S_o (38.1 mm) and S_i (19.05 mm) are the outer and inner spans.

The Slow Crack Growth parameters n and D were then determined by a linear regression analysis using log strength values over the complete range of individual log stress rates, based on the following equation.

$$\log \sigma_f = \frac{1}{n+1}\log \dot{\sigma} + \log D \qquad 1$$

The slope of the linear regression line can be calculated as:

$$\alpha = \frac{K\sum_{j=1}^{K}\left(\log \dot{\sigma}_j \log \sigma_j\right) - \left(\sum_{j=1}^{K}\log \dot{\sigma}_j \sum_{j=1}^{K}\log \sigma_j\right)}{K\sum_{j=1}^{K}\left(\log \dot{\sigma}_j\right)^2 - \left(\sum_{j=1}^{K}\log \dot{\sigma}_j\right)^2} \qquad 2$$

Where α = slope, **K** is the total number of specimens tested (=8), $\dot{\sigma}_j$ and σ_j is the stress rate and fracture strength of the individual test specimen respectively.

The SCG parameter ***n*** is calculated as

$$n = \left(1/\alpha\right) - 1 \qquad 3$$

The intercept of the linear regression line is calculated as

$$\beta = \frac{\left(\sum_{j=1}^{K} \log \sigma_j\right)\sum_{j=1}^{K}\left(\log \dot{\sigma}_j\right)^2 - \left(\sum_{j=1}^{K} \log \dot{\sigma}_j \log \sigma_j\right)\left(\sum_{j=1}^{K} \log \dot{\sigma}_j\right)}{K\sum_{j=1}^{K}\left(\log \dot{\sigma}_j\right)^2 - \left(\sum_{j=1}^{K} \log \dot{\sigma}_j\right)^2} \qquad 4$$

The plot of the log of e flexural strength as a function of log stress rate is shown in fig 4. The SCG parameters n and D were calculated as 23.57, 94.71 and 11.28, 80.2 in air at room temperature and in N_2/Air at 1000ºC respectively.

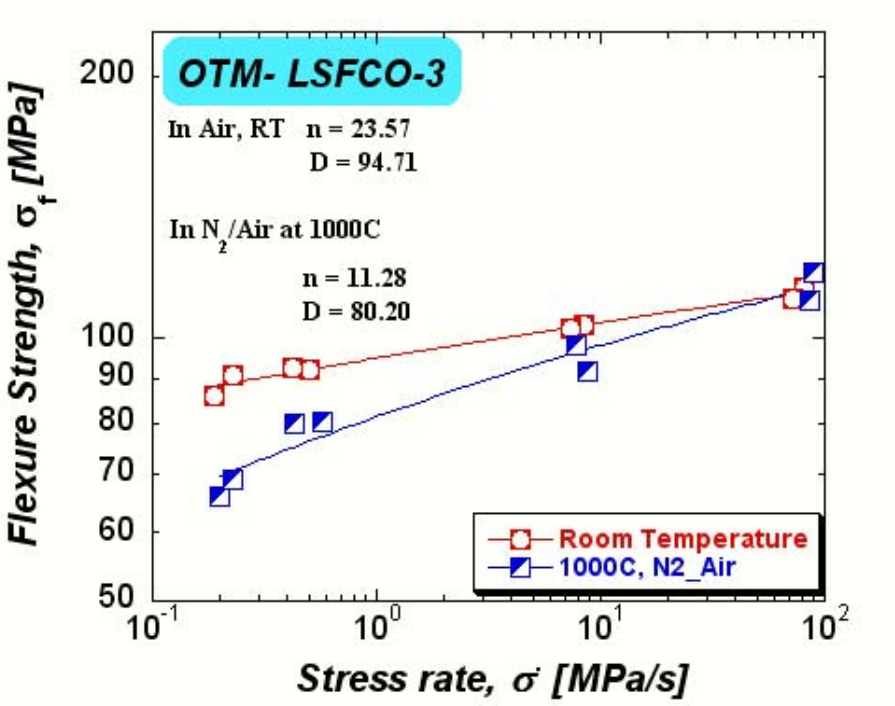

Figure 4 Flexure strength as a function of stress rate (log/log plot).

The high value of n = 23.6 at RT, air indicates that the OTM material is not very susceptible to slow crack growth. However, the value of n decreases drastically to 11.3 in N_2/Air (less than

50% at RT) indicating that the OTM material is prone to SCG. A value of n ≈ 5 or lesser indicates a brittle ceramic which is affected by SCG.

Crack Growth Studies on Indented Samples:

In establishing reliability estimates for a ceramic component, it is very important to have inputs on the structural parameters such as strength and strength distribution (Weibull plots), slow crack growth (SCG) and fracture toughness in the environment. In this quarter, attempts very made to record the fracture toughness in the same environment as in slow crack studies.

Two fracture toughness measurement techniques indentation fracture (IF or IS) and single edge notched beam (SENB) were selected based on their simplicity and ease of testing (fig. 5).

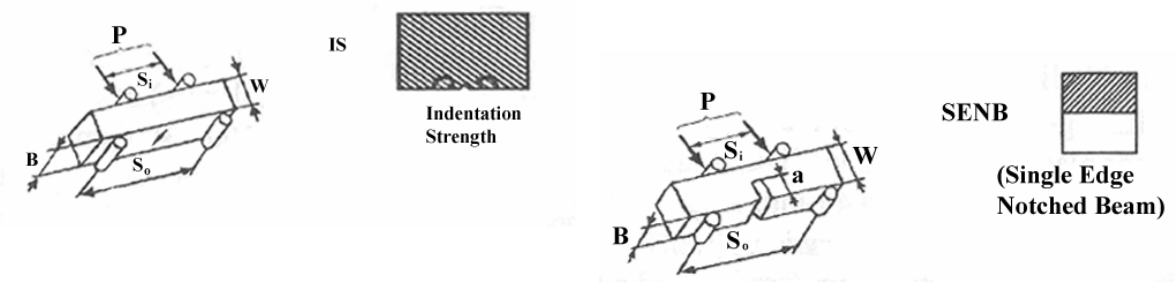

Figure 5 Testing configuration for crack growth studies.

As discussed in previous report, crack healing effects were suspected in the OTM type material and testing in IF method would help in better understanding of the effects. The SENB method relies on a notch introduced in the bar specimen and accordingly a fine notch was created by a 0.075 mm diamond wafering blade.

$$K_{IF} = \frac{3P_{max}\left(S_o - S_i\right)}{2BW^2} \bullet Y\sqrt{a}\ MPa\sqrt{m}$$

The fracture toughness for the IF method, K_{IF} is calculated as: 5

Where Y is the stress intensity factor for the Vickers indent flaw at the surface. Pending detailed observation of fracture in SEM, the Y_{max} is assumed as 1.59.

Two tests were done on the OTM bar specimen. In the first the specimen with a Vickers's indent produced by 9.8 N on the surface was loaded to fracture. As shown in fig. 6, the tests were stopped intermittently and the specimen unloaded. In the second test, the indent introduced on

the surface was polished on a diamond wheel to remove residual surface stress if any. As in the first test, the sample was frequently unloaded to ensure stable crack growth.

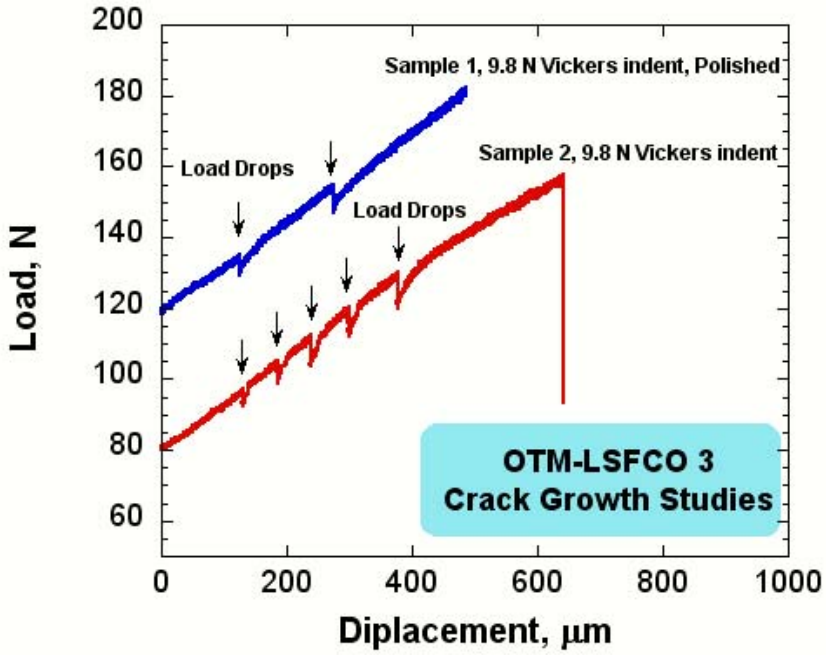

Figure 6 Load-displacement plots for fracture toughness studies in environment.

The fracture toughness for the single edge notched beam (SENB) specimen tested in four-point bending, K_{INB} is calculated using the equations 6 to 7. These equations are valid in the condition 0<a/W<1.

$$K_{INb} = \frac{3P_{max}(S_o - S_i)}{2BW^{3/2}} \bullet \frac{Y_m\left(a/W\right)^{1/2}}{\left(1-a/W\right)^{1/2}} \; MPa\sqrt{m} \qquad 6$$

Where Y_m is the stress intensity factor for the notch of length **'a'** as given by:

$$Y_m = 1.9887 - 1.326\,a/W - \frac{\left(3.49 - 0.68\,a/W + 1.35\,a^2/W^2\right)a/W\left(1-a/W\right)}{\left(1+a/W\right)^2} \qquad 7$$

Fatigue pre-cracking (fig 7) of the notched sample was attempted to convert the SENB test to a more widely accepted single edge pre cracked beam (SEPB) test for ceramics. However, the test frame and the fixture set up were observed to be unsuitable for the low strength OTM materials.

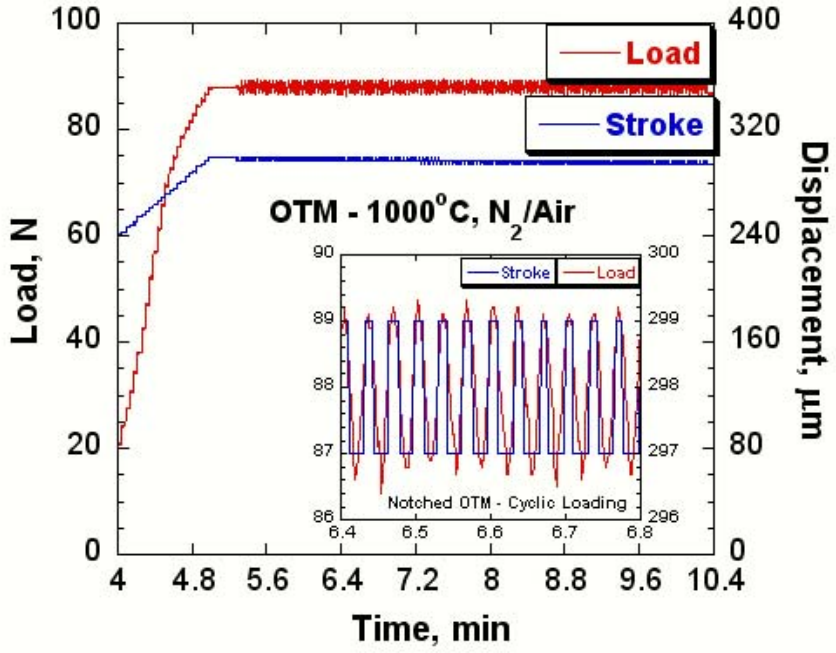

Figure 7 Load-displacement plots for fatigue pre-cracking in environment conditions.

In subsequent studies, alternative techniques such as bridge-compression will be attempted for introducing a sharp pre-crack from the notch.

The fracture toughness of the LSFCO-3 as calculated from the two methods is tabulated in table 4:

Table 4 Fracture toughness (K_c) of OTM (LSFCO-3) in N_2/Air at 1000ºC

Sample No and Configuration	**Load N**	**Outer Span mm**	**Inner Span mm**	**B mm**	**W mm**	**a mm**	**a/W**	**K_C, MPa.m$^{0.5}$**
No. 9 – 2d Surface Crack in Flexure	157.6	38.1	19.05	3.18	4.24	0.15	0.035	1.53
No. 10 – 2e Surface Crack in Flexure – indent Polished	182.4	38.1	19.05	3.25	4.22	0.15	0.035	1.75
No. 11 – 2f Single Edge Notched Beam	92	38.1	19.05	4.04	4.11	1.15	0.28	1.42

At the first take, the fracture toughness of the material recorded from the various techniques appears very similar. However, for proper determination of the toughness careful measurements of the initial crack lengths are to be acquired from the SEM.

Conclusions and future work

Based on the studies and the results presented to Praxair researchers, 8 more OTM (LSFCO-3) samples were provided. Further work will be done to evaluate the fracture toughness in RT, air; N_2/Air at 1000ºC and N_2 at 1000ºC and pressure of 25-50 PSI. Studies will also be done in further reduced environment such as CO_2/Co mixtures.

Fracture of the OTM specimens in air and environment will be analyzed carefully in SEM to delineate SCG and thermal effects. Also, powdered composition will be analyzed in a XRD by slow scans to account for crystal transitions and presence of stresses.

Task 3: Measurement of Surface Activation/Reaction rates in Ion Transport Membranes using Isotope Tracer and Transient Kinetic Techniques.

Prof. Alan Jacobson, University of Houston/University of Toronto

University of Houston

Conductivity and Thermodynamic Studies

We have continued to investigate the thermodynamic properties (stability and phase separation behaviour) and total conductivity of prototype membrane materials. The data are needed together with the kinetic information to develop a complete model for the membrane transport. We have previously reported characterization and conductivity measurements for samples of $La_{0.2}Sr_{0.8}Fe_{0.55}Ti_{0.45}O_{3-x}$. In this report, we describe measurements of the stoichiometry as a function of temperature and pO_2.

Coulometric Titration Experiments

The oxygen non-stoichiometry (δ) for $La_{0.2}Sr_{0.8}Fe_{0.55}Ti_{0.45}O_{3-\delta}$ was measured as a function of oxygen partial pressure at $750 \leq T \leq 1040$ °C. Measurements were made in a sealed electrochemical cells at $10^{-16} \leq pO_2 \leq 0.3$ atm. The measurements were repeated with three different cells. About 0.2~0.5 g of powder was used and measurements made on both decreasing and increasing pO_2. In the beginning of measurements, the relative δ-values as a function of pO_2 were obtained and then the leakage through 8-mol % YSZ leakage corrected over the measured pO_2 ranges. The leakage is more significant at higher temperature and at lower pO_2. Details of the leakage correction procedures have been described previously.

The leakage corrected relative stoichiometry data were normalized as follows. According to Wagner, the minimum value of $\partial\delta/\partial pO_2$ indicates the stoichiometric composition of the sample at this pO_2. That is, in $La_{0.2}^{3+}Sr_{0.8}^{2+}Fe_{0.55}^{3+}Ti_{0.45}^{4+}O_{3-\delta}$, an inflection in the titration data indicates the $\delta \cong 0.175$. One example measured at 950°C is shown in Fig. 8. The solid line in this graph is $\partial\delta/\partial pO_2$. The minimum value of $\partial\delta/\partial pO_2$ at 950°C was found at $pO_2 \sim 8.3 \times 10^{-11}$ and 3.2×10^{-10} atm for high to low and low to high pO_2 measurements, respectively.

The absolute δ-values were obtained with this assumption and the other data points were normalized over the pO_2 range. The entire set of coulometric titration data at different temperatures are shown in Fig. 9. The experimental results display good reproducibility irrespective of the pO_2 direction of measurement. They changed very systematically as a function of temperature and the oxygen partial pressure. The δ-values increased almost linearly on lowering pO_2 until they approached the ideal stoichiometric composition, $\delta = 0.175$. Next, a flat region follows between $pO_2 \sim 10^{-12}$ and 10^{-7} atm. The pO_2 corresponding to the ideal stoichiometry moved to the high pO_2 side as temperature increased. Then, δ-values increased again at further lowering pO_2 regions with a small gap, especially at $pO_2 \leq 10^{-13}$ atm and at $T \geq 1000$ °C.

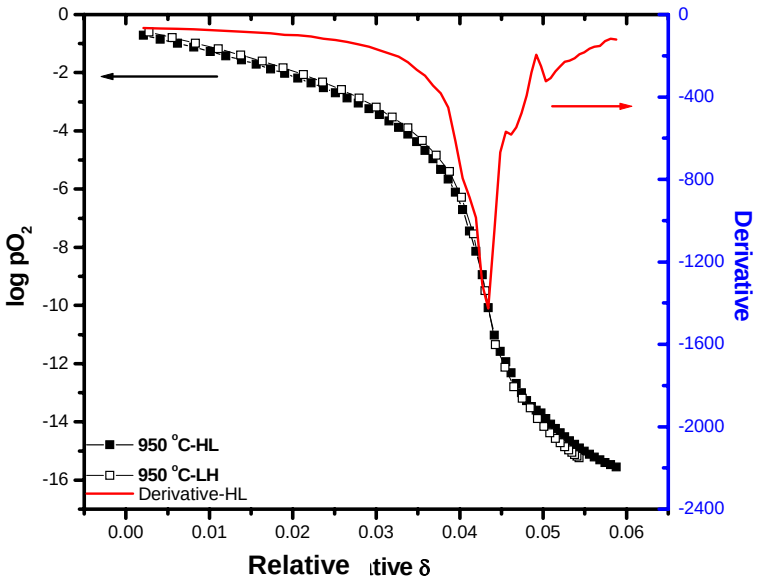

Figure 8 Determination of stoichiometric composition by using the minimum value of $\partial\delta/\partial pO_2$ for $La_{0.2}Sr_{0.8}Fe_{0.55}Ti_{0.45}O_{3-\delta}$ at 950 °C.

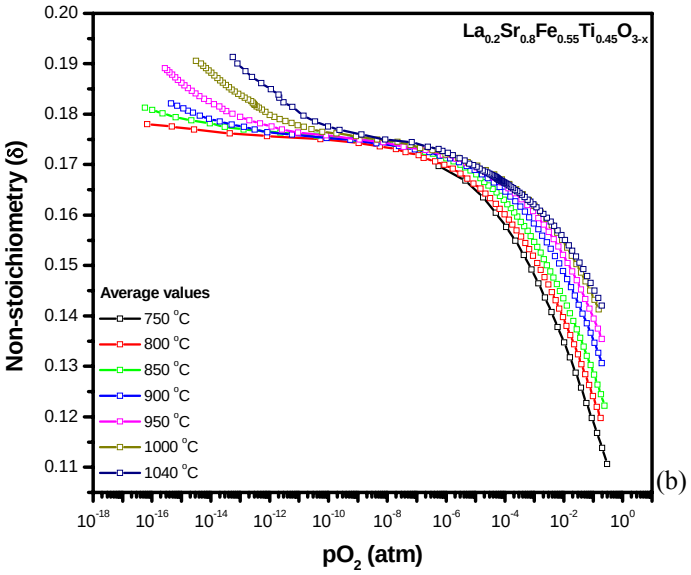

(b)

Figure 9 Average stoichiometry data.

The total changes in δ were less than ~ 0.1 at the pO_2 and temperatures measured. All the normalized experimental results were taken as an average of the data with two measurement directions. All measurements covered the whole pO_2 range except for the low pO_2 values at 750 °C where equilibrium times were too long. These reverse S-shape curves are typical of the coulometric titration experiments. The oxygen non-stoichiometric results can be fitted by using polynomial fitting and the results used to investigate the relationships of δ vs. T at constant pO_2 and log pO_2 vs. T at constant δ.

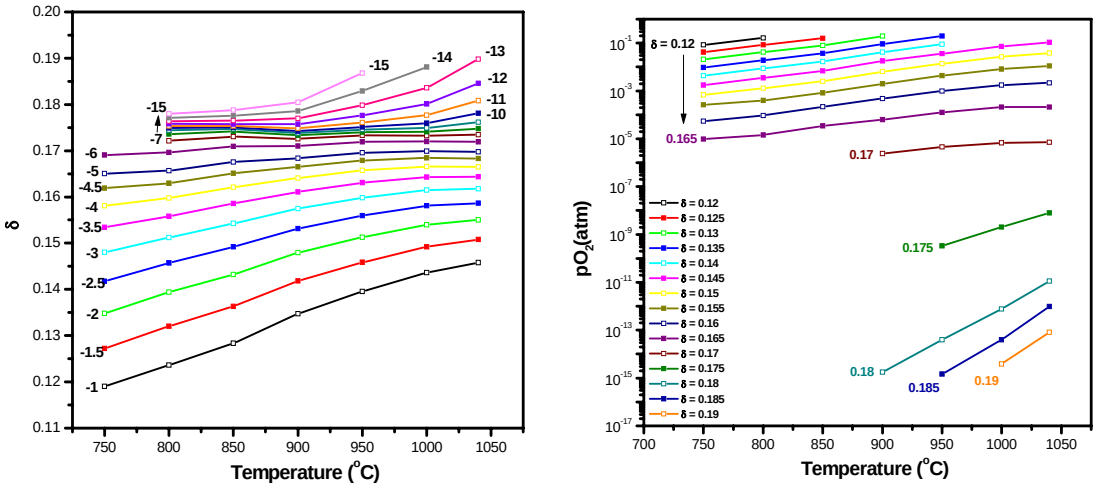

Figure 10 The δ dependence on temperature at constant pO_2 (left) and the pO_2 dependence on temperature at constant δ (right).

The δ dependence on temperature at constant pO_2 is shown in Fig. 10. Equivalent log pO_2 lines are shown for specific values of log pO_2. The lines gradually closer on going from the lower pO_2 side to log pO_2 ~ -6 atm and they become very close together between –7 and –15 atm. The pO_2 dependence on temperature at constant δ is also shown in Fig. 10.

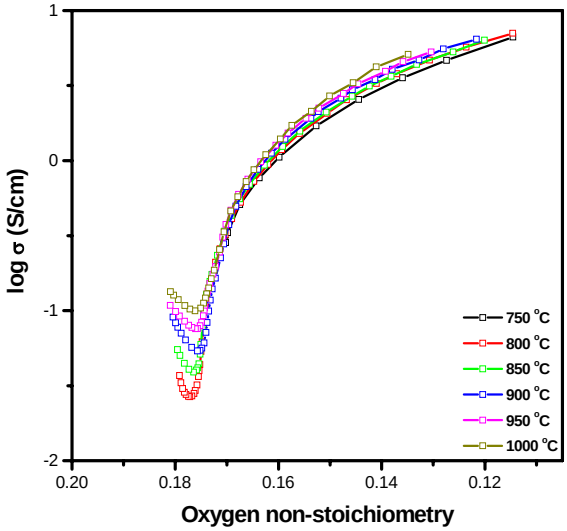

Figure 11 Dependence of conductivity on oxygen non-stoichiometry

We have previously reported the conductivity of $La_{0.2}Sr_{0.8}Fe_{0.55}Ti_{0.45}O_{3-\delta}$ as a function of pO_2 and the pO_2 dependence of the oxygen non-stoichiometry (δ) is described above. These two sets of data were combined and the conductivities plotted as a function of δ in Fig. 11. The p-n

transitions in the conductivity isotherm occur at the compositions $La_{0.2}Sr_{0.8}Fe_{0.55}Ti_{0.45}O_{2.823 \sim 2.824}$ in the temperature range of $800 \leq T \leq 1000$ °C.

Plans for next quarter.

We will extend studies of the $La_{0.2}Sr_{0.8}Fe_{0.55}Ti_{0.45}O_{3-x}$ sample to include measurements of electrical conductivity relaxation to determine the diffusion and the surface exchange coefficients and complete the analysis of the stoichiometry and conductivity data.

University of Toronto

Isotope Transient Studies Through a Dense $La_{0.2}Sr_{0.8}Cr_{0.2}Fe_{0.8}O_{3-\delta}$ Membrane

Summary of experimental progress:

Our last report described the last experiments on LSCF-6428, including the quenching of the sample during the final transient and subsequent cross-sectional analysis by SIMS. We had also just installed a new membrane of $La_{0.2}Sr_{0.8}Cr_{0.2}Fe_{0.8}O_{3-\delta}$ (LSCrF-2828). During the past quarter we have done the following:

The data from the LSCF-6428 study is being re-analyzed in the light of heterogeneities in the membrane which were revealed in the quench experiment. The shapes of the transients on this particular membrane were difficult to fit by the 1-D model and we are currently fitting the data with a two-region model based on the quench results. These exercises are ongoing at the present.

A series of isotope transients under air separation mode (small gradient) were performed on a membrane of LSCrF-2828 at 900°C. These results have been analyzed and are presented below.

A low pO_2 atmosphere has been successfully admitted to the delivery side of the LSCrF-2828 membrane and we are currently operating in a "model syngas" mode and will be performing isotope transients on this membrane under these high gradient conditions.

The table below shows the initial analytical results for the isotope transients on LSCrF-2828 under air separation conditions. The isotope transients were all performed at 900°C. The shapes of the transients were reasonably well fit with the 1-D model, indicating that the membrane does not contain serious flaws or radial heterogeneities.

Isotope transient results for LSCrF-2828

Exp. #	Exp. Condition	k_f, cm/s (x 10^{-5})	(rA)	D, cm^2/s (x 10^{-7})
LSCF-307 Air20|| He (5+20) 900 ºC	1.77%O_2, 0.22%N_2 J_{O2}=0.27 ml/min.cm^2 6 min's pulse (20 ml/min)	1.69	0.77	2.36
LSCF-312 Air20|| He (5+5) 900 ºC	2.71%O_2, 0.48%N_2 J_{O2}=0.16 ml/min.cm^2 6 min's pulse (10.7 ml/min)	1.94	0.86	2.22
LSCF-313 Air20|| He (5+80) 900 ºC	0.51%O_2, 0.06%N_2 J_{O2}=0.27 ml/min.cm^2 6 min's pulse (13.5 ml/min)	1.92	0.76	2.5
LSCF-315 5.1%O_2/N_2/He20|| He (5+20) 900 ºC	0.74%O_2, 0.20%N_2 J_{O2}=0.11 ml/min.cm^2 6 min's pulse (21 ml/min)	0.57	0.67	3.33
LSCF-316 100%O_2 20|| He (5+20) 900 ºC	2.14%O_2, 0.19%N_2 J_{O2}=0.328 ml/min.cm^2 6 min's pulse (18 ml/min)	2.25	0.75	2.22
LSCF-317 Air20|| ***3%O2/He(5+20)*** 900 ºC	3.15%O_2, 8.00%N_2 J_{O2}=0.18 ml/min.cm^2 6 min's pulse (17.5 ml/min)	1.53	0.8	2.78

The values, k_f and r_A, are the forward surface exchange coefficient and the reversibility of the surface exchange ($r_A = k_{reverse}/k_f$) under steady state oxygen permeation conditions. All the values are substantially reversible. The experiments involved variations in the oxygen partial pressure of oxygen on the air side, as well as variations in the He sweep rate on the delivery side. The values of D form a tight grouping near 2.5 x 10^{-7} cm^2/s, with the exception of the 5% oxygen experiment.

Extrapolation of the previous IEDP measurements to 900 ºC , (The highest temperature studied in the IEDP experiments was 850 ºC) shows reasonable consistency with the values under steady state operation under a mild gradient. We are continuing to analyze the transients to place error estimates on the model parameters. This membrane is not perfectly centrosymetric, with the wall thickness varying by 15% radially, and this fact will be included in our further modeling. One final experiment involved the introduction of CO_2 to the delivery side to investigate the effects of

carbon dioxide on that surface process. A reduction in the oxygen flux through the membrane was noted.

"Syngas experiments"

We have just begun to operate the LSCrF-2828 membrane in model "syngas" conditions with a mixture of CO_2/CO on the delivery side. The initial experiments feed a 9%CO,1%CO2 mixture. The oxygen flux is measured by the sum of (1) the change in the CO_2/CO ratio and (2) any molecular oxygen present in the sweep-side gas. The oxygen flux is higher under the initial condition, but these are experiments in progress.

Plans for the next quarter:

Analysis of data: We have been concentrating on data collection for the past few months. Thus much of the analysis has stopped at a cursory stage which (1) assures us of the quality of the data and (2) allows initial evaluation of trends to guide the experiments through a given set of experiments and suggest experiments to complete a give set and guard against omissions of important experiments. In the next quarter, we will pay closer attention to the data analysis of both the final LSCF-6428 and the current LSCrF-2828 data. A visiting student from Technical University, Munich, Stefan Gruber, who will arrive in February, will be asked to polish our 2-D model and revisit the past suite of data.

Syngas experiments: We will be concentrating on the model syngas experiments in the next month. Variations in CO_2/CO ratio and sweep rate will be performed to investigate their effect on oxygen flux. Isotope transients will be performed an many of these conditions. The rapid exchange of carbon dioxide with the perovskite, revealed in our early IEDP measurements, requires us to analyze CO_2 , CO and oxygen for isotope content. Also as revealed in our earlier measurements, the isotope fraction in the CO will reveal the redox exchange part of these surface reactions under steady state. Possibly during the next quarter, we will also introduce hydrogen to the syngas side, to investigate the relative rates of hydrogen and CO oxidation on the delivery side.

CONCLUSIONS

The neutron diffraction data and subsequent refinement indicated an anomalous finding, the Fe/Ti ratio in Ti^{3+} doped $La_{0.6}Sr_{0.4}FeO_{3-\delta}$apparently changes with heat treatment. This is physically possible if there is phase separation (which is not observed in the neutron data). It may however also be a refinement artifact perhaps arising from improper choice of space group. Further analysis using improved neutron diffractometery and Reitveld refinement on a variety of space groups including cubic and tetragonal groups need to be carried out to understand the hysteresis curve for LSF and LSCF series. The studies need to be correlated with the transport and thermal expansion measurements on Ti doped LSF.

For OTM material (LSFCO-3) at room temperature in air, the highest strength of 115 MPa was recorded at the highest cross- head speed of 0.01 mm/s. At elevated temperature (1000ºC) and in an environment of N_2 changing to air), the strength (110 and 118 MPa at high cross-head speeds of 0.01 mm/s) recorded was comparable to that of at room temperature (so called `inert' strength). Thereafter the strength decreased much steeper as indicated by a recorded strength of 69 MPa at 0.00005 mm/s. The SCG parameters n and D were calculated as 23.57, 94.71 and 11.28, 80.2 in air at room temperature and in N_2/Air at 1000ºC respectively. The high value of n = 23.6 at RT, air indicates that the OTM material is not very susceptible to slow crack growth. However, the value of n decreases drastically to 11.3 in N_2/Air (less than 50% at RT) indicating that the OTM material is increasingly prone to SCG. A value of $n \approx 5$ or lesser indicates a brittle ceramic which is affected by SCG. In absence of electron microscopy, initial attempts to record the fracture toughness in the same environment as in slow crack studies remained inconclusive. A low and high of 1.42 and 1.75 $MPa.m^{0.5}$ respectively were recorded from two different techniques.

The oxygen non-stoichiometry (δ) for La0.2Sr0.8Fe0.55Ti0.45O3-δ was measured as a function of oxygen partial pressure at $750 \leq T \leq 1040$ °C. It was noted that the δ-values changed very systematically (total changes in δ were less than ~ 0.1) as a function of temperature and the oxygen partial pressure. The oxygen non-stoichiometric results can be fitted by using polynomial fitting and the results used to investigate the relationships of δ vs. T at constant pO2 and log pO2 vs. T at constant δ.

REFERENCES

N/A

BIBLIOGRAPHY:

N/A

LISTS OF ACRONYMS AND ABBREVIATIONS:

OTM	Oxygen Transport Membrane
LSFCO	Lanthanum Strontium Iron Chromium Oxide ($La_{0.2}Sr_{0.8}Fe_{0.8}Cr_{0.2}O_{3-\delta}$)
LSF	Lanthanum Strontium Ferrite ($La_xSr_{1-x}FeO_{3-\delta}$)
LSCF	Lanthanum Strontium Cobalt Iron Oxide ($La_xSr_{1-x}Fe_{1-y}Co_yO_{3-\delta}$)
L2SF55T	Lanthanum Strontium Iron Titanium Oxide ($La_{0.2}Sr_{0.8}Fe_{0.55}Ti_{0.45}O_{3-\delta}$)